Springer

Journal of Mechanical Science and Technology 22 (2008) 2163~2170

Journal of Mechanical Science and Technology

www.springerlink.com/content/1738-494x
DOI 10.1007/s12206-008-0749-2

Tolerance effects on natural frequencies of multibody systems undergoing constant rotational motion †

Seung Man Eom[1], Bum Suk Kim[2] and Hong Hee Yoo[2]

[1]*Korea Institute of Aerospace Technology, Daejeon, Korea, 305-811*
[2]*School of Mechanical Engineering, Hanyang University, Seoul, Korea, 133-791*

(Manuscript Received February 18, 2008; Revised May 9, 2008; Accepted July 31, 2008)

Abstract

A general multi-body formulation to analyze the tolerance effects on the statistical property variations of natural frequencies of multi-body systems undergoing constant rotational motion is proposed in this paper. To obtain the tolerance effects, Monte-Carlo simulation method is conventionally employed. However, the Monte-Carlo simulation has serious drawbacks; spending too much computation time for the simulation and achieving very slow convergence around some dynamically unstable regions. To resolve such problems, a method employing analytical sensitivity information is suggested in this paper. To obtain the sensitivities of natural frequencies the eigenvalue problem should be differentiated with respect to a design variable. The sensitivities of mass and stiffness matrices should be calculated at the dynamic equilibrium. By employing the sensitivities of natural frequencies along with the tolerance of the design variable, the statistical property variations of the natural frequencies can be calculated.

Keywords: Tolerance; Natural frequency; Dynamic equilibrium; Sensitivity analysis; Multi-body system; Statistical property

1. Introduction

In a state of dynamic equilibrium of a multi-body system, some of the generalized coordinates remain constant while the others vary with time. The dynamic equilibrium states often occur in multi-body systems undergoing constant rotational motion. Such systems can be found in several rotating systems such as a governor mechanism and turbo-machineries-machinery. A formulation to obtain the dynamic equilibrium position of a multi-body system undergoing rotational motion was presented by Choi et al. [1]. The modal characteristics of a multi-body system in dynamic equilibrium differ from those of the same system in static equilibrium. Methods to find the modal characteristics of a multi-body system in static and dynamic equilibriums were proposed by Sohoni and Whitesell [2] and Choi et al. [3], respectively. To design a multi-body system, the static and the dynamic equilibriums and the corresponding modal characteristics at the equilibrium position need to be found effectively as well as accurately. Very often, engineers also need to find the tolerance effects of some design parameters on the statistical property variations of modal characteristics of multi-body systems. Such information is often crucial for the robust design of the a mechanical system.

The effects of various manufacturing tolerances and errors on the motion errors of mechanical systems have been studied by many previous engineers. Hartenberg and Denavit [4] first addressed the issue of mechanical errors in linkages. They estimated the mechanical errors based on the maximum allowable tolerances of the link lengths in four-bar linkages. Their approach employed a deterministic method and offered a "worst case" analysis of tolerance. Garrett

† This paper was recommended for publication in revised form by Associate Editor Seockhyun Kim

*Corresponding author. Tel.: +82 2 2220 0446, Fax.: +82 2 2293 5070
E-mail address: hhyoo@hanyang.ac.kr

and Hall [5] developed a statistical method to determine mechanical errors due to tolerances and clearances and represented the errors as mobility bands. They carried out Monte Carlo simulations for a four-bar linkage with the method. Dubowsky and Freudenstein [6] developed a concept of impact pair and Dubowsky [7] later presented a prediction model for the dynamic effects of clearances in planar mechanisms through the use of the impact pair concept. Lee [8] proposed an effective link model and an analytic method which uses the first-order Taylor series expansion. Lee and Gilmore [9] later considered the uncertainty due to pin location, link length tolerance, and radial clearance tolerance as an effective variation on the link length.

Most of the studies mentioned so far focus on the joint clearance and contact modeling issues and little work has been done to analyze the modal characteristic variations due to design variable tolerances. The purpose of this study is to propose a systematic method to find the statistical property variations of natural frequencies due to design variable tolerances for multi-body systems in dynamic equilibrium. The statistical property variations of natural frequencies are calculated with the sensitivities of natural frequencies, which can be obtained by using the sensitivities of mass and stiffness matrices. A general multi-body formulation is employed to obtain the sensitivities of mass and stiffness matrices.

2. Equations of motion

The most general form of equations of motion for a constrained multi-body system expressed by employing Cartesian coordinates is written (see [10]) as follows:

$$\mathbf{M}\ddot{\mathbf{x}} + \mathbf{\Phi}_{\mathbf{x}}^{T}\boldsymbol{\lambda} = \mathbf{Q} \tag{1}$$

where $\mathbf{M}$ denotes the mass matrix, $\mathbf{Q}$ denotes the generalized force vector, $\mathbf{\Phi}_{\mathbf{x}}$ denotes the Jacobian matrix obtained by differentiating the constraint equations $\mathbf{\Phi}$ with respect to Cartesian coordinates $\mathbf{x}$, and $\boldsymbol{\lambda}$ denotes the Lagrange multiplier vector.

Since the relative configuration of a multi-body system becomes stationary in a dynamic equilibrium state, it is more efficient to employ a set of relative coordinates to describe the system, which is hereafter denoted as $\mathbf{q}$. To derive the equations of motion for a constrained multi-body system by employing a set of relative coordinates, the following equation, which is often called the velocity transformation (see [11, 12]), is employed.

$$\dot{\mathbf{x}} = \mathbf{B}\dot{\mathbf{q}} \tag{2}$$

where $\mathbf{B}$ denotes the velocity transformation matrix, $\dot{\mathbf{x}}$ denotes the system Cartesian velocity vector and $\dot{\mathbf{q}}$ denotes the relative velocity vector.

The relative coordinates $\mathbf{q}$ can be partitioned into $\mathbf{q}_P$ (the coordinates which involve with constant rotational motion) and $\mathbf{q}_R$ (the rest of the relative coordinates) as follows:

$$\mathbf{q} = \begin{bmatrix} \mathbf{q}_P^T & \mathbf{q}_R^T \end{bmatrix}^T \tag{3}$$

Now the Cartesian velocity vector $\dot{\mathbf{x}}$ can be represented in terms of $\dot{\mathbf{q}}_P$ and $\dot{\mathbf{q}}_R$ as follows:

$$\dot{\mathbf{x}} = \mathbf{B}_P\dot{\mathbf{q}}_P + \mathbf{B}_R\dot{\mathbf{q}}_R \tag{4}$$

where $\mathbf{B}_P$ and $\mathbf{B}_R$ denote the sub-matrices associated with the coordinates $\mathbf{q}_P$ and $\mathbf{q}_R$. Thus, $\mathbf{B}$ is composed of $\mathbf{B}_P$ and $\mathbf{B}_R$ as follows:

$$\mathbf{B} = \begin{bmatrix} \mathbf{B}_P & \mathbf{B}_R \end{bmatrix} \tag{5}$$

By taking the time derivative of Eq. (4) one obtains

$$\ddot{\mathbf{x}} = \mathbf{B}_P\ddot{\mathbf{q}}_P + \mathbf{B}_R\ddot{\mathbf{q}}_R + \dot{\mathbf{B}}_P\dot{\mathbf{q}}_P + \dot{\mathbf{B}}_R\dot{\mathbf{q}}_R \tag{6}$$

Substituting Eqs. (6) into Eq. (1) and premultiplying the result by $\mathbf{B}_R^T$, the equations of motion for an open loop system can be obtained as follows:

$$\mathbf{M}^*\ddot{\mathbf{q}}_R = \mathbf{Q}^* \tag{7}$$

where

$$\mathbf{M}^* = \mathbf{B}_R^T\mathbf{M}\mathbf{B}_R \tag{8}$$

$$\mathbf{Q}^* = \mathbf{B}_R^T(\mathbf{Q} - \mathbf{M}\mathbf{B}_P\ddot{\mathbf{q}}_P - \mathbf{M}\dot{\mathbf{B}}_P\dot{\mathbf{q}}_P - \mathbf{M}\dot{\mathbf{B}}_R\dot{\mathbf{q}}_R) \tag{9}$$

3. Deriving linear equations of motion at the dynamic equilibrium state

At the dynamic equilibrium state $\dot{\mathbf{q}}_R$ and its time derivatives $\ddot{\mathbf{q}}_R$ become zero. Also $\ddot{\mathbf{q}}_P$ becomes

zero since $\dot{\mathbf{q}}_P$ is prescribed constant. So, from Eq. (7), the following dynamic equilibrium equation can be obtained.

$$\mathbf{B}_R^T(\mathbf{M}\dot{\mathbf{B}}_P\dot{\mathbf{q}}_P - \mathbf{Q}) = \mathbf{0} \tag{10}$$

Since the above equation is nonlinear in terms of $\mathbf{q}_R$, it can be solved by employing an iterative numerical scheme such as the Newton-Raphson method.

Now, Eq. (7) can be expressed in a more general form as follows:

$$g(\ddot{\mathbf{q}}_R, \dot{\mathbf{q}}_R, \mathbf{q}_R, \dot{\mathbf{q}}_P, t) = 0 \tag{11}$$

If Equation (11) is linearized at the dynamic equilibrium positions (which is denoted as $\mathbf{q}_R^*$) the following equation can be obtained.

$$\delta g = \left.\frac{\partial g}{\partial \ddot{\mathbf{q}}_R}\right|_{\mathbf{q}_R^*} \delta\ddot{\mathbf{q}}_R + \left.\frac{\partial g}{\partial \mathbf{q}_R}\right|_{\mathbf{q}_R^*} \delta\mathbf{q}_R = 0 \tag{12}$$

Eq. (12) may be rewritten in a familiar form as

$$\hat{\mathbf{M}}\delta\ddot{\mathbf{q}}_R + \hat{\mathbf{K}}\delta\mathbf{q}_R = 0 \tag{13}$$

where $\hat{\mathbf{M}}$ and $\hat{\mathbf{K}}$, respectively, denote the linearized mass and stiffness matrices, that are written as

$$\hat{\mathbf{M}} = \left.\frac{\partial g}{\partial \ddot{\mathbf{q}}_R}\right|_{\mathbf{q}_R^*} = \mathbf{B}_R^T\mathbf{M}\mathbf{B}_R\big|_{\mathbf{q}_R^*} \tag{14}$$

$$\hat{\mathbf{K}} = \left.\frac{\partial g}{\partial \mathbf{q}_R}\right|_{\mathbf{q}_R^*} = \frac{\partial}{\partial \mathbf{q}_R}\mathbf{B}_R^T[\mathbf{M}\mathbf{B}_P\dot{\mathbf{q}}_P - \mathbf{Q}]\big|_{\mathbf{q}_R^*} \tag{15}$$

4. Analysis of the tolerance effect on the natural frequency variance using the sensitivity information

An Eigenvalue problem of an undamped system can be written as follows:

$$\hat{\mathbf{K}}\phi_j = \lambda_j\hat{\mathbf{M}}\phi_j \tag{16}$$

where ϕ_j denotes the normalized mode vector and λ_j denotes the eigenvalue.

Now differentiating Eq. (16) with respect to a design variable b, one may obtain obtains

$$(\hat{\mathbf{K}} - \lambda_j\hat{\mathbf{M}})\frac{\partial\phi_j}{\partial b} = -(\frac{\partial\hat{\mathbf{K}}}{\partial b} - \lambda_j\frac{\partial\hat{\mathbf{M}}}{\partial b})\phi_j + \frac{\partial\lambda_j}{\partial b}\hat{\mathbf{M}}\phi_j \tag{17}$$

Pre-multiplying Eq. (17) by ϕ_j^T and using the normalized condition $\phi_j^T\hat{\mathbf{M}}\phi_j = 1$, the sensitivity of an eigenvalue λ_j for a design variable b can be obtained as follows:

$$\frac{\partial\lambda_j}{\partial b} = \phi_j^T(\frac{\partial\hat{\mathbf{K}}}{\partial b} - \lambda_j\frac{\partial\hat{\mathbf{M}}}{\partial b})\phi_j \tag{18}$$

Since $\lambda_j = \omega_j^2$, the sensitivity of a natural frequency ω_j for a design variable b can be obtained as follows:

$$\frac{\partial\omega_j}{\partial b} = \frac{1}{2\omega_j}\phi_j^T(\frac{\partial\hat{\mathbf{K}}}{\partial b} - \lambda_j\frac{\partial\hat{\mathbf{M}}}{\partial b})\phi_j \tag{19}$$

When a set of samples of a design variable has a normal distribution with 99.73% confidence interval, the variance of the natural frequency (see Ref. [8]) can be obtain obtained as

$$\sigma^2 = \frac{1}{9}\left(\frac{d\omega_j}{db}\right)^2 T^2 \tag{20}$$

where T denotes the tolerance of the design variable b and σ denotes the standard deviation of the natural frequency ω_j.

5. Numerical examples

5.1 Rotating simple pendulum

Fig. 1 shows the rotating simple pendulum undergoing rotational motion with constant angular velocity Ω. The pendulum (mass m=3kg and length L=1m) is connected to a vertical shaft by a pin joint as shown in the figure. When the vertical shaft rotates with a constant angular velocity, θ remains constant at the dynamic equilibrium position. Fig. 2 shows the dynamic equilibrium value of θ versus the angular velocity. Until the shaft angular velocity exceeds the value of 3.835rad/s, the dynamic equilibrium value of θ remains zero, since the virtual moment generated by the gravitational force is larger than that generated by the centrifugal force. Fig. 3 shows the natural fre-

quency versus the angular velocity. As the shaft angular velocity increases, the natural frequencies decreases first and then increases. Especially, the natural frequency reaches zero at 3.835rad/s since the system stiffness becomes zero at the angular velocity. Fig. 4 shows the mean value of the natural frequency versus the angular velocity when the length of bar has the a normal distribution with 99.73% confidence interval. Three tolerances are considered: 3.0%, 6.0% and 12.0%. As shown in the plot, there is little difference between the results obtained by the proposed method and the analytical solution for the three cases of tolerances.

Fig. 5 shows the a comparison of standard deviations of the natural frequency obtained by three methods: the proposed method, Monte-Carlo method, the analytical method. For the analysis, the length of the pendulum is assumed to have the a tolerance of 3%.

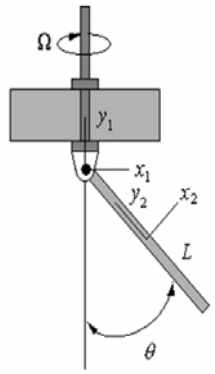

Fig. 1. Rotating simple pendulum system.

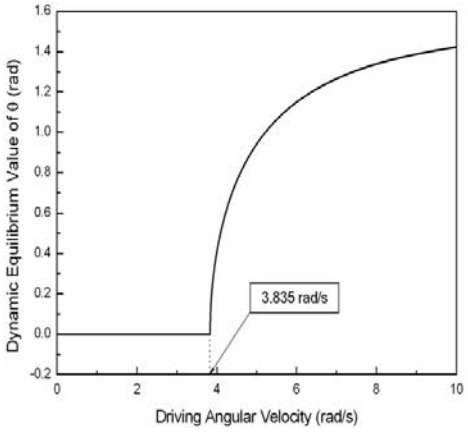

Fig. 2. Dynamic equilibrium value of θ versus the angular velocity.

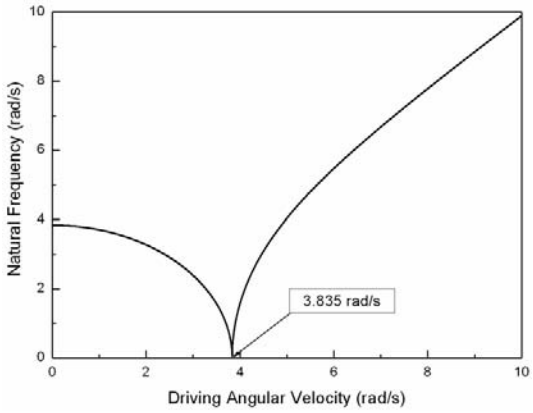

Fig. 3. Natural frequency versus the angular velocity.

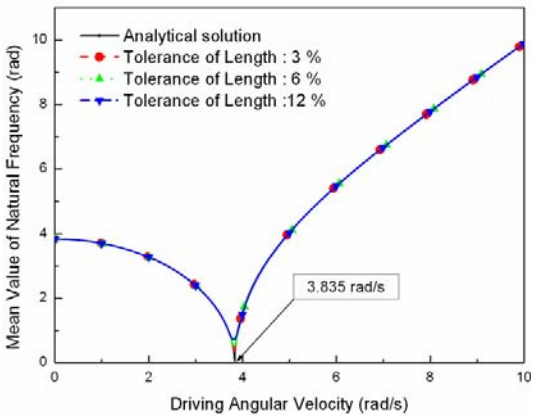

Fig. 4. Mean value of natural frequency versus the angular velocity.

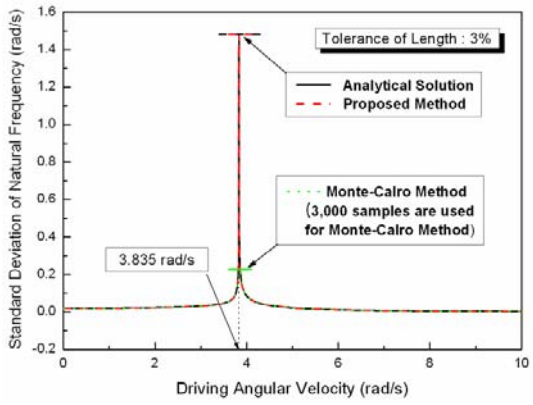

Fig. 5. Comparison of standard deviations obtained by the proposed method and the Monte-Carlo method.

Table 1. Comparison of CPU time between the proposed method and the Monte-Carlo method.

Method	CPU Time (sec)	Ratio
Proposed Method	1.328	1
Monte-Carlo Method	1565.797 (0.435 hours)	1179

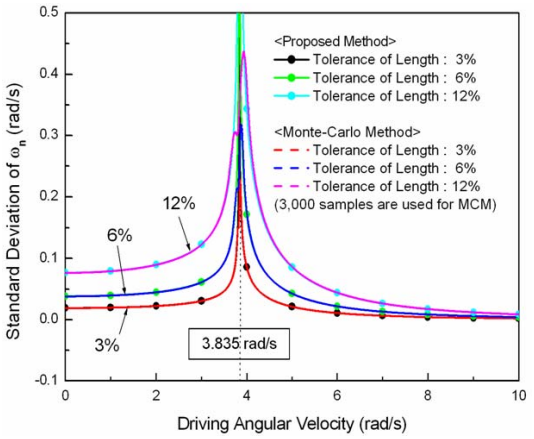

Fig. 6. Comparison of the standard deviations with three different tolerances.

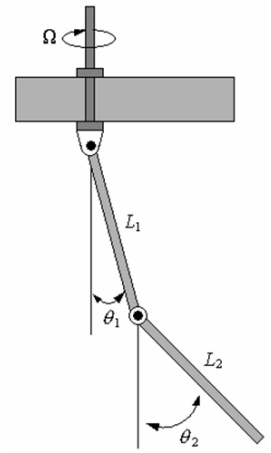

Fig. 7. Rotating double pendulum system.

As shown in the figure, the standard deviation becomes large around the angular velocity 3.835rad/s at which the natural frequency becomes null. The results obtained by the analytical solution are in good agreement with those obtained by the proposed method. However, they do not match to the results obtained by the Monte-Carlo method around the angular velocity 3.835rad/s.

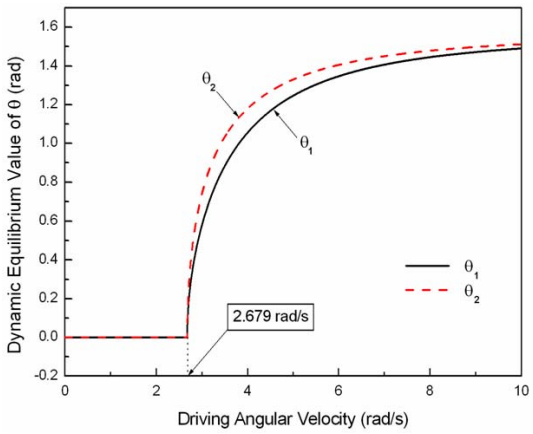

Fig. 8. Equilibrium angles versus the angular velocity.

Fig. 6 shows the standard deviation of natural frequency versus the angular velocity with three cases of tolerances: 3.0%, 6.0% and 12.0%. As inspected intuitively, the deviation increases as the tolerance increases.

Table 1 shows the comparison of CPU time between the proposed method and the Monte-Carlo method. A standard Pentium PC is employed for the calculation. As shown in the table, the computation time consumed by the proposed method is less than a thousandth of that consumed by the Monte-Carlo method.

5.2 Rotating double pendulum

Fig. 7 shows a rotating double pendulum system which rotates with a constant angular velocity. The mass and the length of the two pendulums which are mutually connected by a rotational joint are 3kg and 1m, respectively. The first pendulum is also connected to the vertical shaft which rotates with a constant angular velocity relative to the ground. The angle between the vertical shaft and the first pendulum is denoted as θ_1 and the angle between the first pendulum and the second pendulum is denoted as θ_2.

Fig. 8 shows the values of the two angles at the dynamic equilibrium state versus the angular velocity. As shown in the figure, those two equilibrium angles remain 0 until the angular velocity reaches 2.679 rad/s. After exceeding the angular velocity, the virtual moment generated by the centrifugal force becomes lager larger than that generated by the gravitational force. As the angular velocity increases, those two angles converge to $\pi/2$ radian.

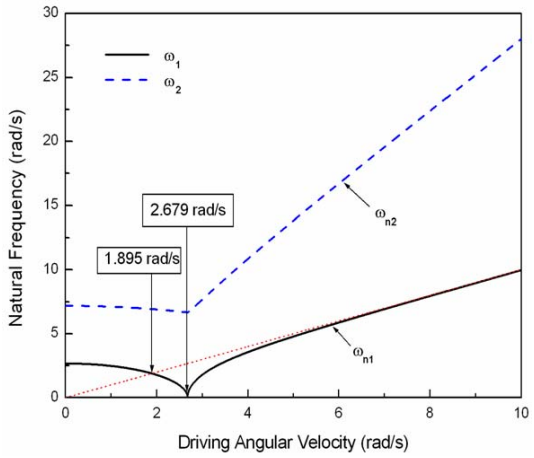

Fig. 9. Variations of natural frequencies versus the angular velocity.

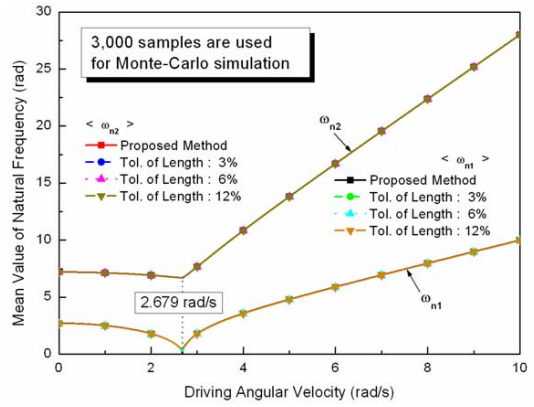

Fig. 10. Mean values of natural frequencies versus the angular velocity.

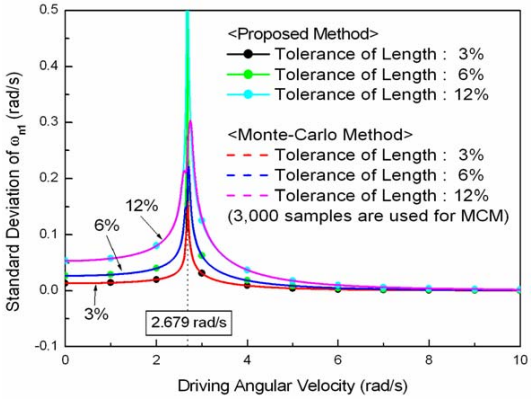

Fig. 11. Comparison of the first natural frequency standard deviations obtained by the proposed method and the Monte-Carlo method.

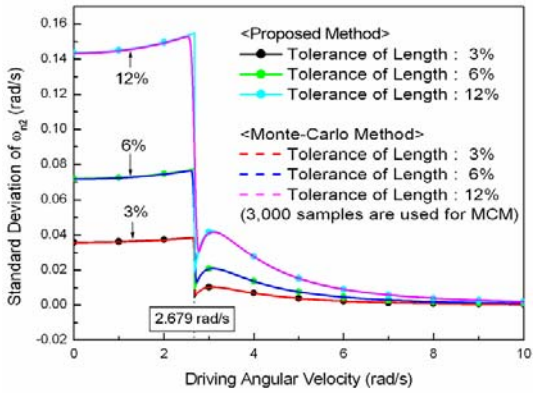

Fig. 12. Comparison of the second natural frequency standard deviations obtained by the proposed method and the Monte-Carlo method.

Fig. 9 shows the variations of the first and the second natural frequencies versus the angular velocity. The natural frequencies decrease first, then increase. The driving angular velocity is the same as the natural frequency on the dotted red line. As shown in Fig. 9, the angular velocity matches to the first natural frequency at 1.895rad/s. Since a resonance may occur at the angular velocity, it is often called a critical angular velocity. As shown in the figure, the first natural frequency becomes 0 when the angular velocity becomes 2.679 rad/s. So the system becomes unstable at the angular speed, too.

Fig. 10 shows the mean values of the first and the second natural frequencies obtained by the proposed method and the Monte-Carlo simulation. For the Monte-Carlo simulation 3,000 samples were employed to draw the figure. As shown from the figure, the two methods provide almost identical results. It can be also observed from the results that the mean values of the natural frequencies rarely vary as the tolerance increases.

Fig. 11 and Fig. 12 show the standard deviations of the first and the second natural frequencies versus the angular velocity, respectively. The results obtained by the proposed method and the Monte-Carlo method are in a good agreement, except the specific angular velocity region (near 2.679 rad/s). It was shown from theThe previous results showed that the first natural frequency becomes null at the angular velocity. Especially, as shown in Fig. 11, significant error occurs for the first natural frequency standard deviation at the angular velocity. For the second natural frequency standard deviation, however, the error is not significant. As inspected intuitively, the natural frequency

Table 2. Comparison of CPU time between the proposed method and the Monte-Carlo method.

Method	CPU Time (sec)	Ratio
Proposed Method	11.297	1
Monte-Carlo Method	15979. (4.4386 hours)	1414

standard deviations increase in proportional to the tolerance of the design variable. Incidentally, it can be also found that the error remains insignificant at the critical angular velocity where the first natural frequency matches to the angular velocity.

Table 2 shows the a comparison of CPU time between the proposed method and the Monte-Carlo method. It can be found from the table that the proposed method is computationally much more efficient than the Monte-Carlo method. One should note that the computation time for the double pendulum system is more than 4 hours. So if the Monte-Carlo method is employed for a more practical multi-body system example, the computational burden becomes prohibitive.

6. Conclusions

The following summary and conclusions could be obtained from this study.

- A general multi-body formulation to investigate the design variable tolerance effect on the statistical property variations of natural frequencies is proposed by employing the sensitivity information.
- The proposed method is computationally much more efficient than the Monte-Carlo method so that it can be employed for more practical design problems of constrained multi-body systems.
- Compared to the Monte-Carlo method, the proposed method can always provide more accurate results. It was shown that the Monte-Carlo method often provides erroneous results around a certain angular velocity region

References

[1] D. H. Choi, J. H. Choi, J. H. Park and H. H. Yoo, "Steady-State equilibrium analysis of a multibody system driven by constant generalized speeds," *KSME International Journal,* 16 (10) (2002) 1239-1245.

[2] V. N. Sohoni and J. Whitesell, Automatic linearization of constrained dynamical models, *ASME Journal of Mechanisms, Transmissions, and Automation in Design* , 108 (1986), 300-304.

[3] D. H. Choi, J. H. Park and H. H. Yoo, Modal analysis of constrained multibody systems undergoing rotational motion, *Journal of Sound and Vibration*, 208 (1) (2005), 63-76.

[4] R. S. Hartenberg and J. Denavit, *Kinematic synthesis of linkages*, McGraw-Hill, New York, USA, (1964).

[5] R. E. Garret and A. S. Hall, Effects of tolerance and clearance in linkage design*, ASME Journal of Engineering for Industry*, 91 (1969) 198-202.

[6] S. Dobowsky and F. Freudenstein, Dynamic analysis of mechanical systems with clearances, Part 1: Formulation of dynamic model, *ASME Journal of Engineering for Industry*, 90 (1971) 305-316.

[7] S. Dobowsky, On predicting the dynamic effects of clearances in planar mechanisms, *ASME Journal of Engineering for Industry*, 96 (1974) 317-323.

[8] S. J. Lee, Performance reliability and tolerance allocation of stochastically defined mechanical systems, The Pennsylvania State University, Ph.D. Dissertation, (1989).

[9] S. J. Lee and B. J. Gilmore, The determination of the probabilistic properties of velocities and accelerations in kinematic chains with uncertainty, *ASME Journal of Mechanical Design*, 113 (1991), 84-90.

[10] E. J. Haug, Computer-aided kinematics and dynamics of mechanical systems, *VolumnVolume I: Basic Method*, ALLYN AND BACON (1989).

[11] S. S. Kim and M. J. Vanderploeg, A general and efficient method for dynamic analysis of mechanical systems using velocity transformations, *ASME Journal of Mechanisms, Transmissions and Automation in Design*, 108 (1986) 176-182.

[12] D. S. Bae and E. J. Haug, A recursive formulation for constrained mechanical system dnamics : Part I. open loop systems, *Mech. Struct. & Mach*., 15 (3) (1987) 359-382.

[13] C. S. Rudisill, 1974, Derivatives of eigenvalues and eigenvectors of a general matrix, *AIAA Journal*, 12 (1974) 721.

Seung Man Eom graduated from the Department of Mechanical Engineering at Incheon University in 2005 and received his master degree from the Department of Mechanical Engineering at Hanyang University in 2007. He is currently working as a Researcher of Aircraft Development Team in KIAT(Korea Institute of Aerospace Technology, Koreanair), DaejeonDeajeon, Korea.

Bum Suk Kim graduated from the School of Mechanical Engineering at Hanyang University in 2006 and received his master degree from the same department in 2008. He is currently working as a Ph.D. student in the School of Mechanical Engineering in Hanyang University, Seoul, Korea.

Hong Hee Yoo graduated from the Department of Mechanical Design and Production Engineering at Seoul National University in 1980 and received his master degree from the same department in 1982. He received his Ph.D. degree in 1989 from the Department of Mechanical Engineering and Applied Mechanics in the University of Michigan at Ann Arbor, U.S.A. He is currently working as a professor in the School of Mechanical Engineering in Hanyang University, Seoul, Korea.